Chapter 8

Small Punch Creep

Robert J. Lancaster and Spencer P. Jeffs

Additional information is available at the end of the chapter

http://dx.doi.org/10.5772/intechopen.70375

Abstract

A thorough characterisation of the creep properties of any modern alloy designed for a structural application can be an expensive and timely process. As such, significant effort is now being placed in identifying suitable alternative characterisation techniques. The small punch creep (SPC) test is now widely regarded as an effective tool for ranking and establishing the creep properties of a number of critical structural materials from numerous industrial sectors. Over recent years, the SPC test has become an attractive miniaturised mechanical test method ideally suited for situations where only a limited quantity of material is available for qualification testing. Typically, the method requires only a modest amount of material and can provide key mechanical property information for highly localised regions of critical components. As such, SP creep testing offers a feasible option of determining the creep properties of novel alloy variants still at the experimental stage and the residual life of service-exposed material.

Keywords: small punch, creep, fractography, empirical correlations, numerical correlations

1. Introduction

Small punch (SP) test methods were initially developed in the 1980s by the nuclear industry, then known as the miniaturised disc bend test, where it was used to estimate the mechanical properties and residual life of irritated materials [1–3]. It was then in the 1990s that it was proposed the technique could be utilised to establish elevated temperature creep properties of materials [4], from which it has received significant interest in terms of its potential advantages and applications and is now more commonly known as the Small Punch Creep (SPC) test. **Figure 1** demonstrates the continuously growing research and interest in SPC testing by the number of documents listed searching the expression 'small punch creep' in Scopus since 1970 [5].

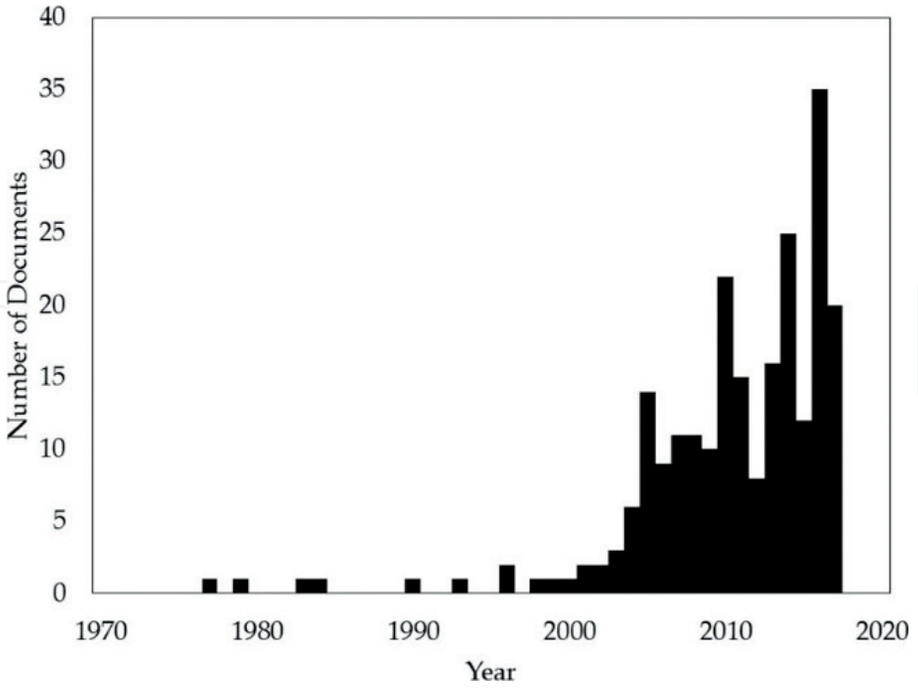

Figure 1. Number of documents listed in Scopus each year where the expression 'small punch creep' is included in the title, abstract or the keywords in the engineering, materials science and energy subject areas [5].

The key feature of the SPC test in comparison to conventional mechanical test methods derives from its use of small disc specimens, the dimensions of which have been seen to be between 3 and 10 mm in diameter and 0.2–0.5 mm in thickness depending on the test being performed [6].

The use of small disc specimens breeds a range of advantages and applications for the SPC method. As was the original intent of its development the technique has found success in remnant life assessment of in-service components such as pressure vessels and boiler pipes [7–9]. Disc specimens for determining remnant life are generally extracted from in-service components by means of scoop sampling [10], a schematic for which is shown in **Figure 2** [11]. This is then typically followed by Electrical Discharging Machining (EDM) and a grinding/polishing process to the desired thickness, thus generating disc samples ready for testing. The different stages of this process for sample preparation are shown in **Figure 3**. Other means of extracting SP discs include EDM directly from components or structures without the necessity of the scoop sampling step or by turning down thread ends from uniaxial specimens on a CNC lathe. In cases where sampling does not compromise the structural integrity of a component, the technique may be considered a Non-Destructive Test (NDT) [12].

Besides its initial development for remnant life assessment, SPC has been proven to be effective at determining localised material behaviours over a range of material systems, processes and engineering sectors. These include:

- In power plants, welding processes are used for the integration of complex pipe systems resulting in the necessity to understand the evolution of properties throughout the base material, weld material and heat-affected zone (HAZ) [13]. As a result, the SPC test has

http://dx.doi.org/10.5772/intechopen.70375

been implemented to assess the creep properties of weldments at high temperatures over a range of materials [13–16].

- In additive manufacturing (AM) processes, such as direct laser deposition (DLD) which is of large interest to the aerospace sector, SPC has enabled mechanical characterisation that may not be possible with conventional test methods due to geometry restrictions. Therefore, SPC has offered the possibility of providing effective ranking of different process variables and orientations on component representative geometries [17]. This principle of ranking through SPC can then be transferred across into early stage alloy development where only limited material stock may be available.
- Changes in mechanical behaviour such as establishing the effect of anisotropy in textured materials [18, 19], identifying grain size sensitivity along with revealing the influence of chemical compositions [20] have been unveiled through the SPC test.

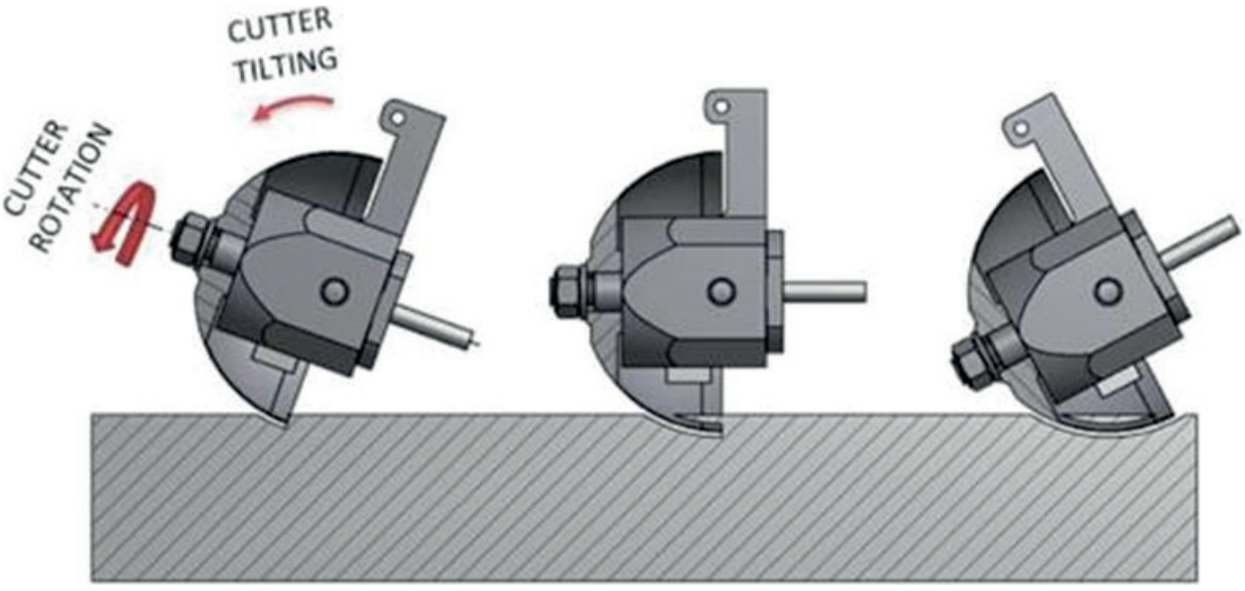

Figure 2. Schematic of scoop sampling process [11].

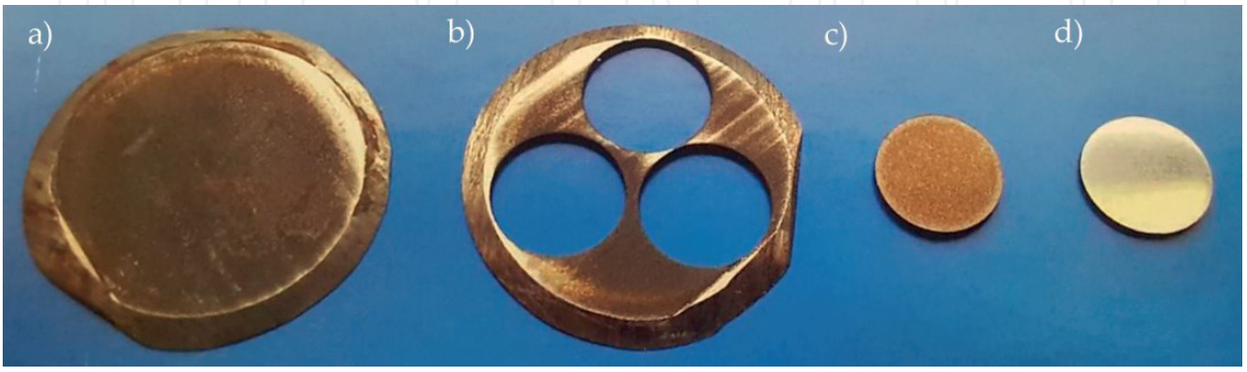

Figure 3. (a) Scoop sample, (b) scoop sample after EDM, (c) SP samples obtained through EDM and (d) polished SP specimen ready for testing.

- Finally, the technique has long been adopted as a means of determining equivalent or correlated uniaxial properties over a wide range of material systems including nickel based single crystal material ®CMSX-4 [21, 22], γ-titanium aluminide [23], aluminium alloys [24] and stainless steel [25].

Overall the technique has been adopted for a variety of research and development purposes to further highlight the range of potential benefits of using miniature disc specimens to derive creep properties of materials. Currently, SPC is undergoing a stringent procedure to progress from a working code of practice [26] into a European standard [27]. This has been supported by the creation of a specialist group of worldwide researchers who are collaborating towards standardising the procedure with a targeted publication date of 2019. This effort is supplemented by round robin testing across different institutions to establish the reliability and repeatability of the technique and confirm its place as an accepted mechanical testing methodology.

2. Experimental procedures

In a small punch creep (SPC) test, a miniature disc specimen with typical dimensions of 8–9.5 mm in diameter and 500 μm in thickness is subjected to a constant load that is applied to the material through a punch indenter. As the load is applied to the disc, the material undergoes a biaxial form of deformation prior to the onset of final rupture.

2.1. Test frame assembly

The SPC test is usually performed in a dead-weight test frame assembly as displayed in **Figure 4**. In this arrangement, the miniature disc is positioned into the recess of a lower die, which locates the specimen in the centre of the rig. The disc is then fixed securely via a circumferential clamping load to prevent any residual flexing of the material during test. However, over clamping should be avoided to reduce any plastic deformation which may influence the final test result. Hand tight clamping is usually suffice to ensure repeatability in results. Loading is then applied through the central axis of the frame via an upper load pan which exerts a force onto the specimen via a punch indenter.

2.1.1. Punch indenter

The punch tip typically consists of a hemi-spherical end with a diameter ranging from 2 to 2.5 mm, but an alternative assembly can also be used such as a flat tip indenter and a 2–2.5 mm diameter ceramic ball. Typical ball materials include Si_3N_4. In this instance, the ball should be replaced after every test. The geometries of the two punch configurations are displayed in **Figure 5**. Depending on the material that is to be tested, the punch material can vary from high strength steel for testing relatively soft and ductile materials such as copper, to high temperature ceramic materials including zirconium oxide and aluminium oxide for testing creep resistant materials such as single crystal alloys. For testing at elevated temperatures, oxidation and wear of the punch is a concern and may require refurbishment after every test.

http://dx.doi.org/10.5772/intechopen.70375

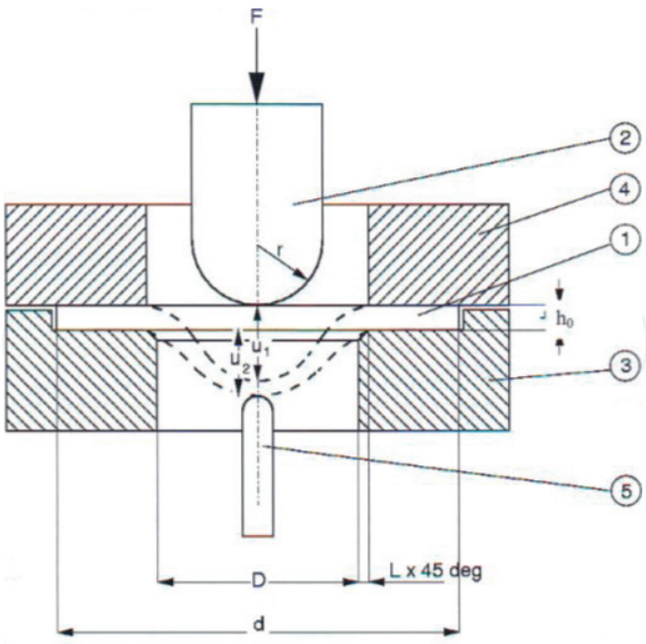

1. SP disc test piece — u_1, u_2 = displacement
2. Hemispherical ended punch — h_0 = 0.5mm
3. Lower Die — d = 8-9.5mm
4. Upper Die — r = 1-1.25mm
5. Transducer quartz rod — D = 4mm

Figure 4. Small Punch Creep Test Set-up [26].

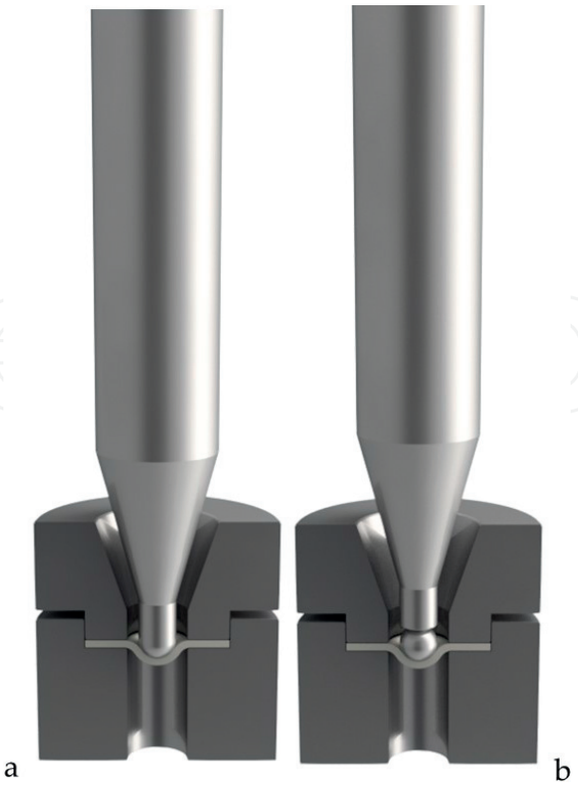

Figure 5. Schematic diagrams of the punch geometries for (a) one piece punch and (b) ball-punch configuration.

2.1.2. Measurement of deformation

Upon exertion of the testing load, disc deformation is monitored and recorded from two locations via linear variable displacement transducers (LVDTs). One LVDT is usually positioned in a location to detect the movement of the load pan and records the displacement on the top surface of the disc. The other LVDT is located within the lower die—pull rod assembly and measures the deflection on the underside surface of the specimen via a quartz rod. This enables the deformation on both surfaces to be closely monitored throughout a test and the resultant SPC curve usually displays an average of the top and bottom recordings.

2.1.3. Heating instrumentation and measurement

In a SPC test, heat is usually applied via a digitally controlled single zone furnace or induction heating and is constantly monitored throughout the test by one or two thermocouples (either type K or N depending on the desired temperature). One thermocouple should be placed in contact with the underside of the disc, with an optional second thermocouple located in a drilled hole in the upper die, close to the top surface of the specimen.

For high temperature SP testing, an inert gas environment is usually recommended to avoid oxidation of the disc specimen.

2.2. Specimen preparation

For SPC testing, disc specimens are usually removed from a larger piece by extracting cylindrical rods of the test material through EDM. The rods are turned down to the desired diameter (8–9.5 mm) and sectioned into slices approximately 800 μm thick. The material is then ground on both faces with progressively finer grit papers until a 500 ± 5 μm thickness is achieved with a 1200 grit finish. The use of smaller test pieces (diameter = 3 mm, thickness = 250 μm) is also permissible to allow the use of TEM specimens. In either specimen geometry, a representative volume must be contained in the thickness of the disc to obtain macroscopic material properties. This would typically include at least five grains in the cross-sectional thickness.

Prior to testing, the disc thickness shall be measured at four locations around the perimeter at 90° intervals to ensure uniformity.

3. Results

The result of a SPC test is characterised by a time-displacement/deflection curve with recognisable stages of deformation, notably primary, secondary and tertiary creep. This behaviour is comparable to that expected from a conventional uniaxial creep test for a given material. However, in reality the actual material deformation is considerably different. In a SPC test, the period of primary creep represents the elastic bending period of disc deformation. This leads to the onset of plastic deformation and membrane stretching under a biaxial stress condition, coinciding with an extended phase of secondary creep. The deformation then continues as the disc starts to experience considerable necking due to thinning, before accelerating to failure, akin to tertiary creep. This contrasts with the behaviour observed in a

traditional uniaxial creep arrangement where the test specimen simply elongates under an applied tensile load with time.

Figure 6a displays a series of typical SPC curves from tests performed on the single crystal superalloy CMSX-4, at 950°C under a variety of applied loads. The same results can also be represented in terms of the minimum displacement rate with time, as shown in **Figure 6b**. In a similar manner to uniaxial creep data, the results can also be plotted in terms of time to rupture, t_f, an example of which is given in **Figure 7**. As the graph shows, SPC testing demonstrates a sensitivity to temperature and loading, as would be expected in conventional creep test results.

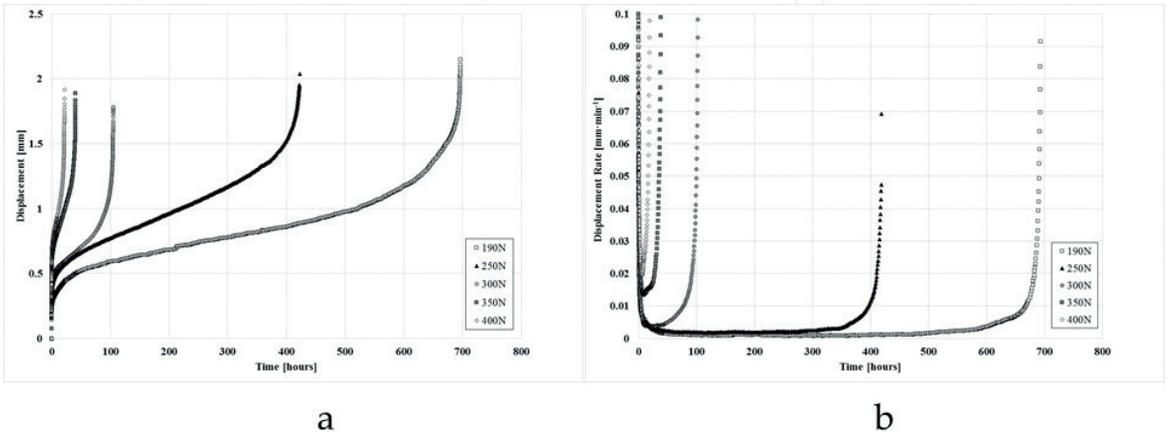

Figure 6. (a) SP creep curves and (b) minimum displacement rates for CMSX-4 tested at 950°C under a range of applied loads [21].

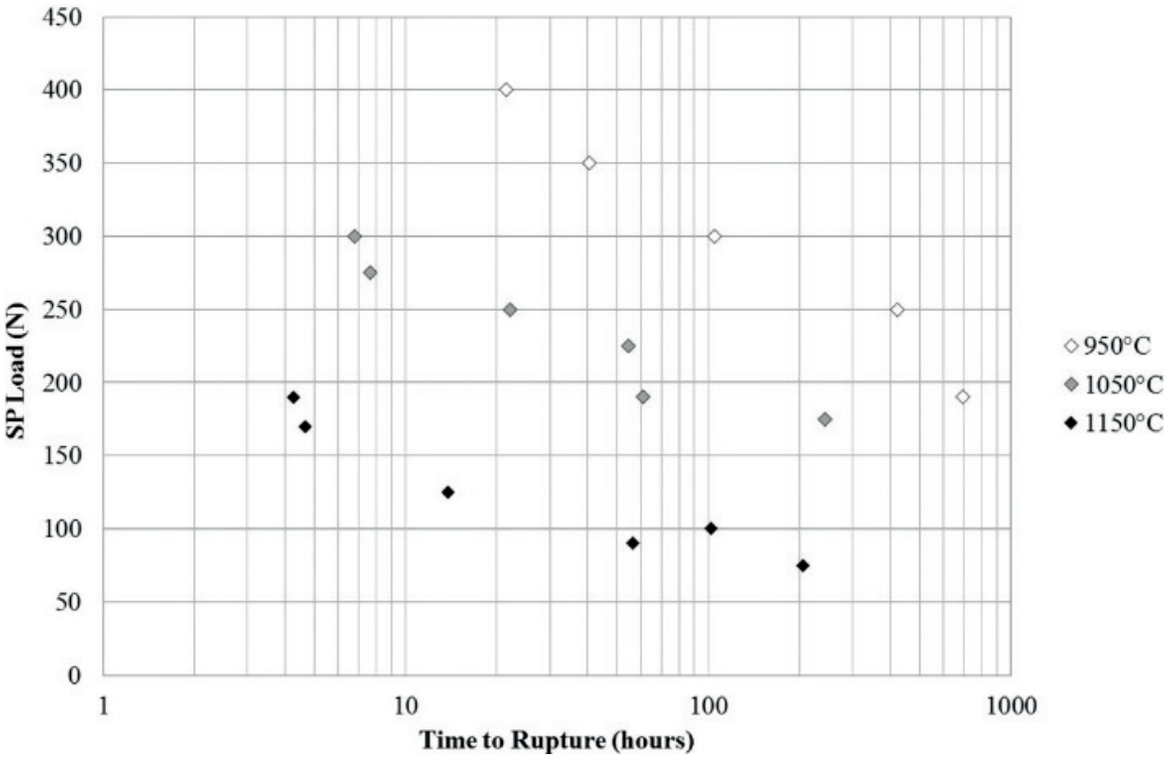

Figure 7. Load vs Time to Rupture for SPC tests on CMSX-4 at 950°C, 1050°C and 1150°C [21].

3.1. Fractography

In a SP creep test, the manner of failure usually resembles one of two dominant modes of fracture; ductile or brittle. In a ductile failure, the fracture usually initiates around the periphery of the punch head in the vicinity of tensile membrane stretching, propagating along the circumference indicating that the maximum stress is found away from the central region of the disc. **Figure 8** illustrates a typical example of a ductile fracture for a ruptured high nitrogenic ferritic steel specimen, tested at 725°C under a load of 140N [28]. The fracture morphology displays a cap-like form of deformation whilst severe necking can be seen around the central region of the disc. The higher magnification image, given in **Figure 8b**, shows a dominant transgranular type behaviour with ductile dimples covering the surface.

In contrast, SP testing has also been employed to characterise the creep properties of more inherently brittle type materials, such as γTiAl [23] or Mg alloys [24].

Figure 9 presents the typical fracture morphology for a brittle small punch disc. In this example, a SP creep test was performed at 650°C on a 14Cr ODS steel, a ferritic/martensitic

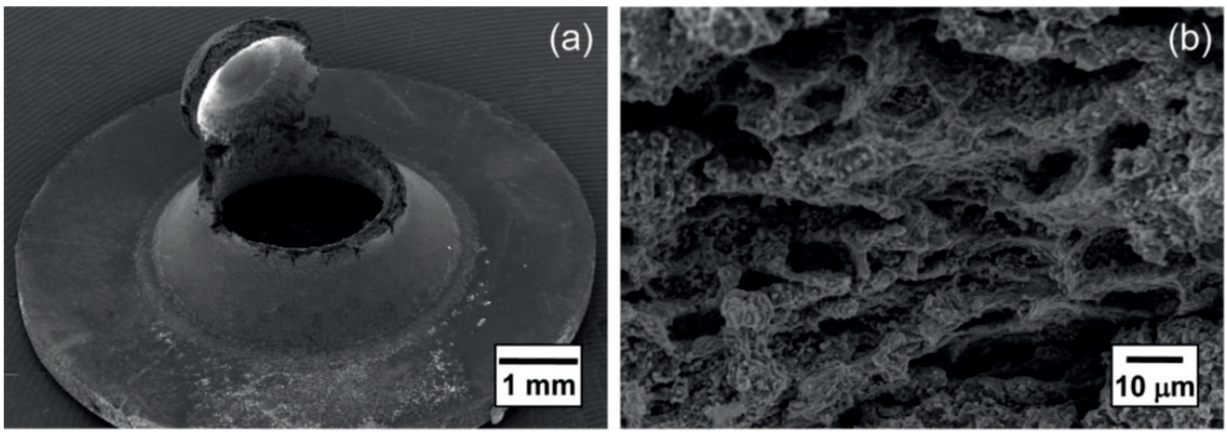

Figure 8. (a) A typical SP creep ductile fracture surface for a test on HN9L at 725°C at 140N and (b) fracture surface depicting ductile transgranular mode of fracture [28].

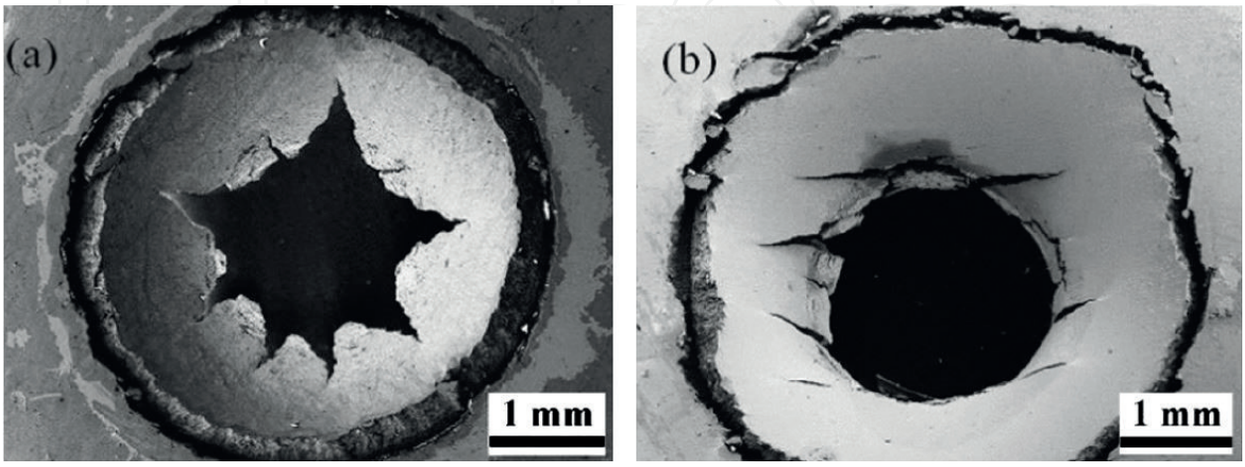

Figure 9. SEM micrographs of SP creep specimens for a 14Cr ODS Steel with a brittle fracture in (a) the transverse orientation and (b) the longitudinal orientation [18].

oxide dispersion strengthened material that exhibits a highly anisotropic microstructure and mechanical response [18].

Figure 9 shows the fracture behaviour in the two specimen orientations denoted as transverse (a) and longitudinal (b). The fracture morphology in the transverse specimen clearly shows radial type cracking emanating from the central point of the disc, in direct contrast to the behaviour seen in a more ductile material. However, in the longitudinal specimen, a series of parallel intergranular cracks can be seen which are aligned to the extrusion process of the material fabrication.

4. Data interpretation and correlations to uniaxial creep results

Previous research [13, 23] has demonstrated that the shape of the time displacement/deflection curves from SP creep tests are qualitatively similar and representative of the shape typically observed from uniaxial testing approaches. Now, over recent years, many researchers and scientists have devoted significant effort in establishing a series of correlative means capable of comparing the results obtained from SP creep testing to data gathered from more traditional creep testing methodologies. These include approaches to obtain equivalent stress values rather than load, strain values rather than deflection/displacement and a minimum creep rate rather than minimum displacement rate.

4.1. Deflection – Chakrabarty membrane stretch model

In 1970, Chakrabarty [29] proposed a theory for a material stretching over a hemispherical punch head, now widely known as the membrane stretch model. This theory has provided the basis for much of the understanding of the relationship between central deflection and strain for a small punch creep test [30]. Assumptions include a rigid punch that is well lubricated so friction is considered negligible, rigid-plastic material due to the large strains and deformation occurring through membrane stresses alone.

Based upon Chakrabarty's model, Li and Šturm [31] devised the following third order polynomial [Eq. (1)] for the equivalent strain at the contact boundary, ε. In this equation, central deflection is given as δ, the receiving hole diameter is 4 mm and the punch radius is 1 mm, as recommended in the European Code of Practice (CoP) for small punch testing [26]. The strain at the contact boundary is considered since necking and failure in SPC are commonly located away from the specimen centre [32].

$$\varepsilon = 0.20465\delta + 0.12026\delta^2 + 0.00950\delta^3 \tag{1}$$

When considering other SPC setups, specifically a punch diameter of 2.5 mm, the constant parameters within the polynomial equation change accordingly [31]. Not only has Chakrabarty's model provided an insight into the strain-deflection relationship, but has further been implemented to help determine the relationship between stress and load with SPC, as discussed further in the k_{SP} method.

Nevertheless, the Chakrabarty model has its limitations in that it is only really suitable for large deformations which is not always the case with brittle materials where specimens may crack upon loading or in the early phase of the test [23], or fractures that reveal a star type pattern as illustrated earlier [18]. In addition, any strain hardening effects must be considered rather than an exponential hardening law only as is the case here [32].

4.2. Empirical approaches

4.2.1. The k_{SP} *method*

The most widely recognised technique for empirical correlation of SP creep and uniaxial results is the SP creep correlation factor, k_{SP}. In this approach, the SP load can be correlated to a uniaxial creep stress to compare the two sets of data, using the following equation [Eq. (2)]:

$$\frac{F}{\sigma} = 3.33 k_{SP} R^{-0.2} r^{1.2} h_0 \tag{2}$$

where F is the SP load, σ is the applied stress in a uniaxial creep test, R is the radius of the receiving hole, r is the radius of the punch indenter and h_0 is the thickness of the disc specimen.

This a $\frac{F}{\sigma} = 3.33 k_{SP} R^{-0.2} r^{1.2} h_0$ approach has been derived from Chakrabarty's membrane stretching theory but remains empirical in nature due to the inclusion of a material constant, represented here as the k_{SP} value. In situations where no uniaxial creep results are available, this value is usually referred to as 1. However, in such instances the method is less reliable and can only serve as a rough approximation of the corrected creep stress.

The k_{SP} method has been successfully applied to several material systems, notably CMSX-4 [21], P91 [33] and P92 [13] steels. **Figure 10** demonstrates the correlation obtained from the technique for P92 steel, both as a base metal and as weld material [13], and for the lightweight aluminium alloy AlSi9Cu3 [24]. In both examples, the results show good agreement between

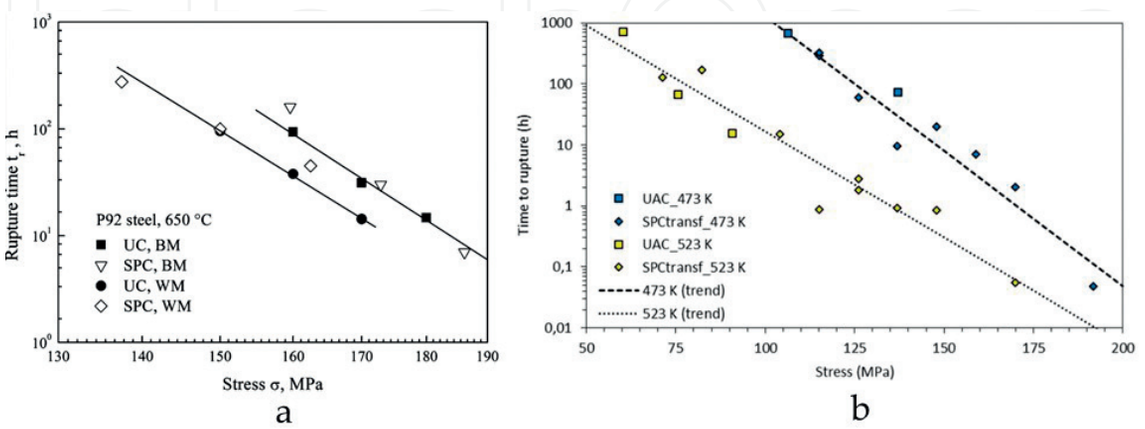

Figure 10. Comparison of uniaxial creep and SPC data using the k_{SP} method for a. P92 steel at 600°C [13] and b. AlSi9Cu3 at 473 and 523K [24].

uniaxial and SPC results but the k_{SP} value was found to change for the base metal (1.035) and weld material (0.977) in P92. This difference is attributed to the higher yield strength observed in the base material, which leads to a change in the manner of deformation.

Conversely, the k_{SP} method has been found to be limited to materials with proven ductility and the correlations for more inherently brittle alloys are not as impressive. **Figure 11** presents the relationship for γTiAl 45-2-2 (XD) [23] at elevated temperatures and a clear breakdown in the correlation is observed. This is related to the use of the k_{SP} value as a ductility factor, and the catastrophic manner in which γTiAl 45-2-2 (XD) was found to crack on the onset of loading during a SPC experiment.

4.2.2. Monkman-Grant

The Monkman-Grant model is a well recognised predictive approach for uniaxial creep data that can also be observed in SPC. The technique typically considers the relationship between t_f and the minimum strain rate, $\dot{\varepsilon}$, but can also be modified to account for SPC when considering the minimum deflection rate $\dot{\delta}_M$, in the form of:

$$\log t_f + m \log \dot{\delta}_M = C_S \tag{3}$$

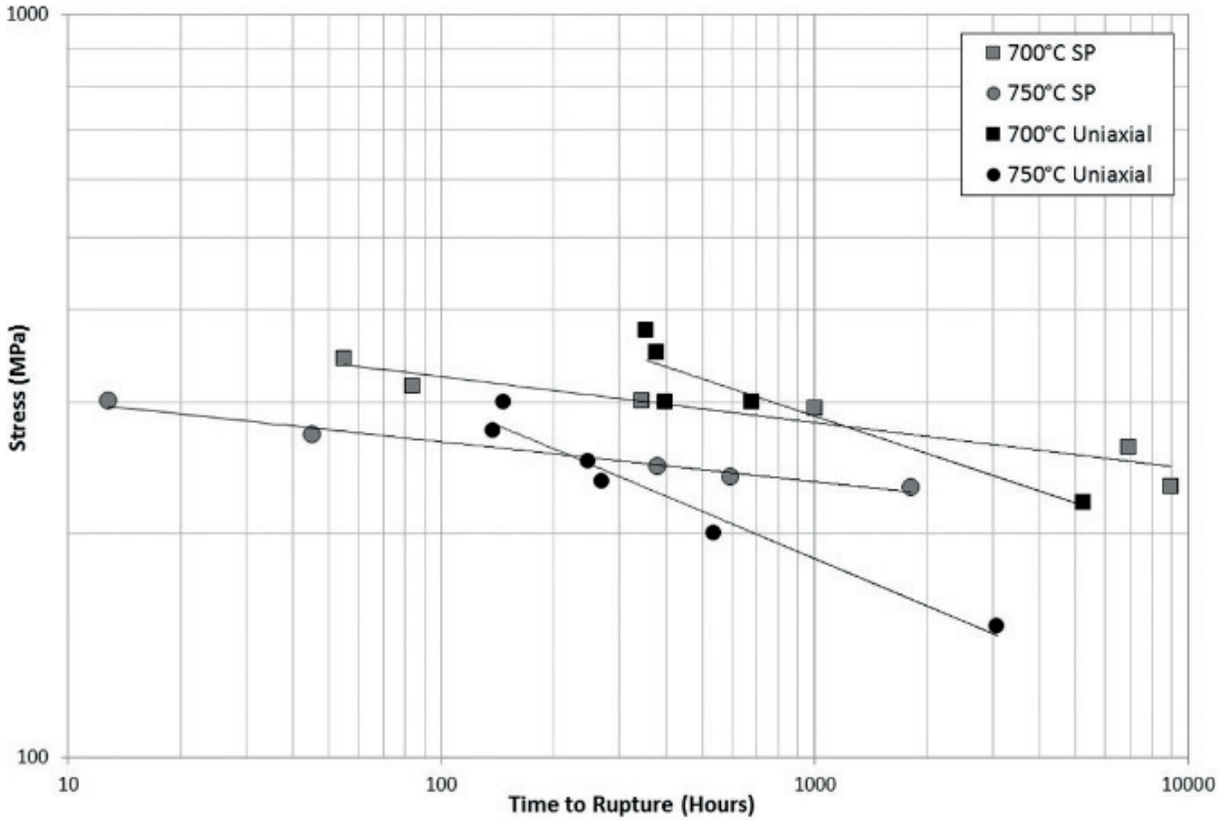

Figure 11. k_{SP} correlation for uniaxial and converted SPC data for γTiAl 45-2-2 (XD) at 700 and 750°C [23].

where C and m are material constants typically defined by linear regression. If the rupture times are equal across the two test types, a correlation may be derived [34] which sanctions a direct comparison of the two rates, $\dot{\varepsilon}$ and $\dot{\delta}_M$, through the following equation:

$$\dot{\varepsilon} = 10^{C - C_{s/m}} \dot{\delta}_M \tag{4}$$

Dobes and Milicka [35] used such a relationship to correlate the minimum creep rate from a uniaxial creep test to the minimum deflection rate from a SPC experiment. Dymáček [36] applied this methodology to P92 NT steel and found parallel trends in the two data sets, demonstrating the applicability of the Monkman-Grant relationship to SPC data (**Figure 12**).

4.2.3. Larson-Miller

The Larson-Miller parameter (LMP) is an established means of predicting the lifetime of materials subjected to creep damage by using a correlative based approach that incorporates the Arrhenius equation. The LMP correlates the relationship between temperature (T), stress and t_f using the following equation:

$$LMP = T\left(C + \log t_f\right) \tag{5}$$

where C is a material constant.

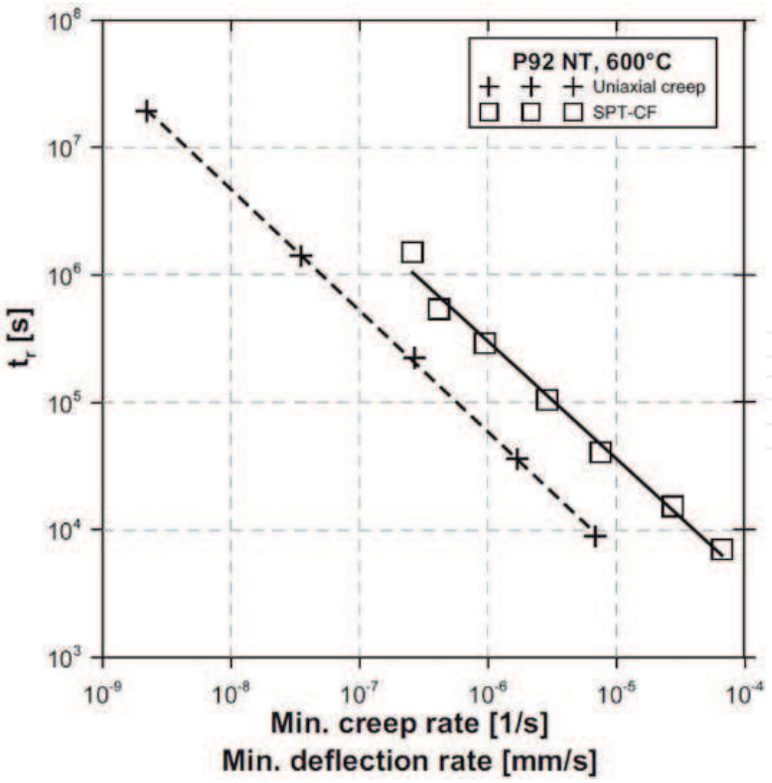

Figure 12. Monkman-Grant relationship for SPC and uniaxial creep results on P92 NT steel at 600°C [36].

A series of researchers [24, 28] have applied the LMP to interpret SPC data, but to also establish a relationship between SPC and uniaxial creep results. Andrés et al. [24] obtained a LMP design curve from SPC results on the magnesium alloy AZ31 through linear regression, once the equivalent uniaxial creep stress was defined. In this research, C was assumed as a constant value to guarantee matching LMP values in both test approaches. The results are illustrated in **Figure 13** which correlates the two data sets and shows good agreement, confirming the suitability of the approach.

4.2.4. Theta projection

The theta-projection approach has found extensive use in the life prediction of uniaxial creep data. The method, developed by Evans and Wilshire [37], has attracted widespread attention [38] and is capable of obtaining an accurate creep deformation curve with a true representation of the three dominant stages of creep. This method can be simplified to accommodate SPC tests via the following expression:

$$\varepsilon = At + B\left(e^{\alpha t} - 1\right) \tag{6}$$

where t is the creep time, A and B are parameters related to the hardening and weakening of strain and α is the constant of creep deformation rate, making the equation more applicable to constant load deformation.

Zheng et al. [39] used this approach to extrapolate the SPC deformation curves of service-exposed Cr5Mo Steel at 550°C, as presented in **Figure 14**, and choose 20% of the creep life as

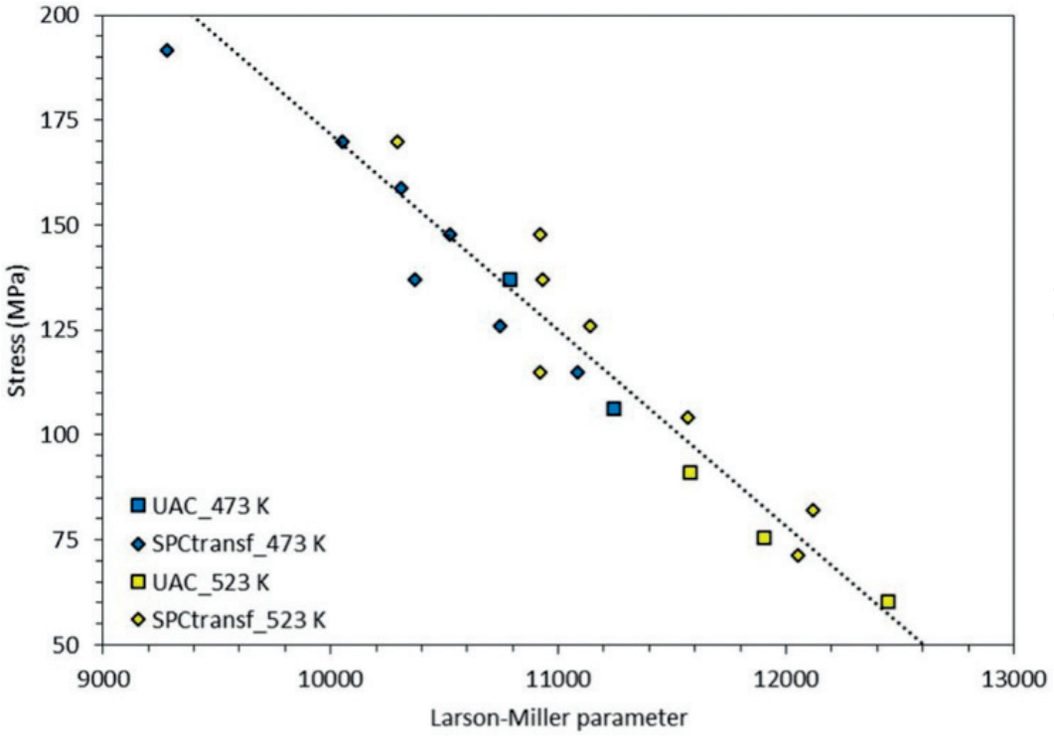

Figure 13. Correlation of SPC equivalent stress to uniaxial creep against LMP for AZ31 alloy [24].

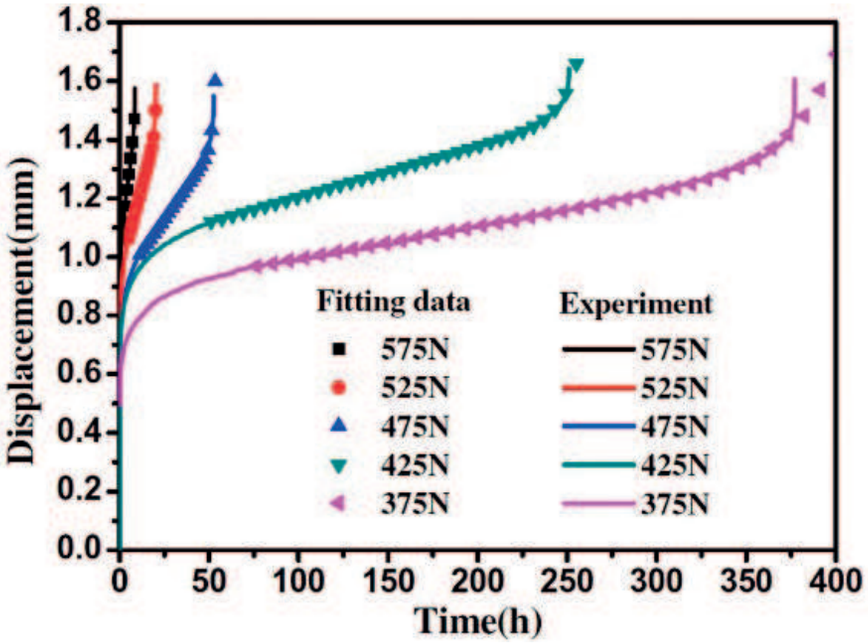

Figure 14. SPC time-deflection fitting curves using the theta-projection method on service-exposed Cr5Mo Steel at 550°C [39].

the starting point for the prediction. As **Figure 14** illustrates, this approach shows good agreement with the generated experimental data

4.2.5. Norton (1/2)

The most important and useful properties from the SPC test are t_f and $\dot{\delta}_M$. In an identical manner to traditional uniaxial creep test approaches, both properties in a SPC test are heavily dependent on the applied test temperature and load. These parameters directly influence the controlling creep mechanism which can vary from diffusional creep to dislocation creep, with dislocation creep more prevalent at higher and intermediary applied stress levels and at temperatures high enough to activate creep (0.4 Tm).

The relationship between $\dot{\delta}_M$ and the applied force F of a SPC test can be described by a power law in a similar manner to the well established Norton law for uniaxial creep approaches, where:

$$\dot{\delta}_M = AF^n \tag{7}$$

Here, A is a proportionality constant. Gülçimen and Hähner [14] used such an approach to determine and compare the local creep properties of a P91 weldment across three distinct zones, namely the base metal, weld metal, and the heat-affected zone. Yang et al [40] also used a similar approach to establish the relationship between $\dot{\varepsilon}$ and $\dot{\delta}_M$, allowing for an approximate conversion of the small punch deflection to the equivalent creep strain in Incoloy880H. **Figure 15** shows the Norton relations for the individual zones in P91 and in Incoloy880H.

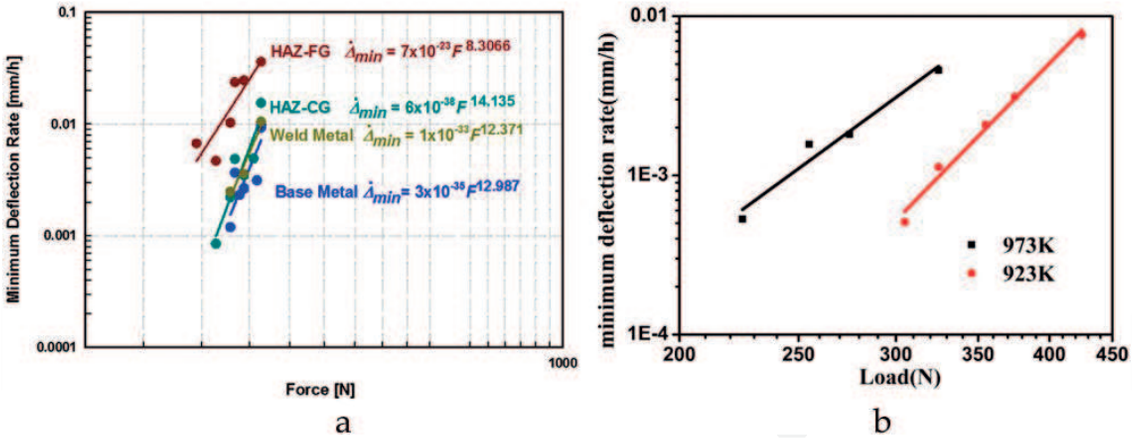

Figure 15. Norton laws for a. base metal, weld metal, HAZ-FG and HAZ-CG in P91 steel [14] and b. Incoloy880H [40].

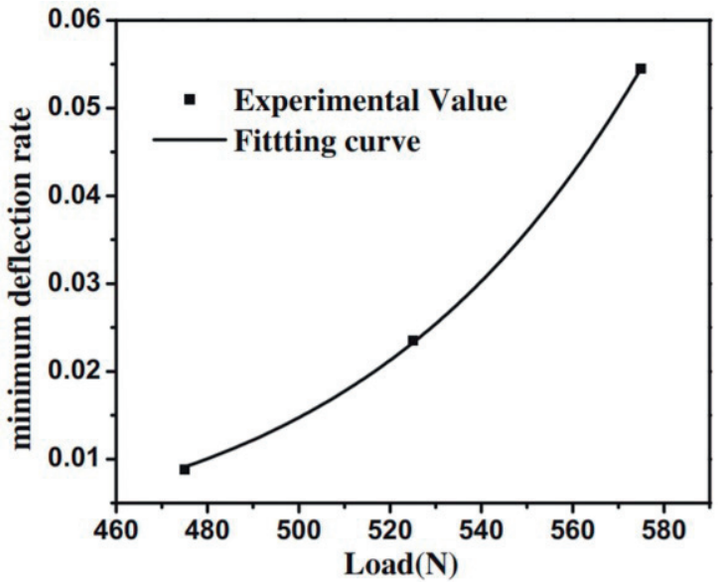

Figure 16. Relationship between minimum deflection rate and load for Cr5Mo steel [39].

Zheng et al. [39] used the Norton relationship to determine the correlation between the stable creep rate and the applied load. This was achieved by using a curve fitting procedure, where the material's $\dot{\delta}_M$ can be predicted from the value of the applied load. The result of this curve fit is displayed in **Figure 16** for Cr5Mo steel. The authors found the prediction represents a 15% error compared to the actual value and can be used as an accurate prediction of the remaining life of the material.

4.2.6. Wilshire equations (1)

The Wilshire equations have been well established over the last few decades and offer the potential to predict long term creep life based on relatively short term creep data [41–43]. The principle is based upon the assumptions that $t_f \rightarrow 0$ as $\sigma \rightarrow \sigma_{TS}$ while $t_f \rightarrow \infty$ as $\sigma \rightarrow 0$, with applied stress, σ, related to t_f through the following equation:

$$(\sigma/\sigma_{TS}) = \exp\left\{-k_1\left[t_f \exp(-Q_c*/RT)\right]^u\right\} \tag{8}$$

where σ_{TS} is the ultimate tensile strength in MPa, Qc^* is the apparent activation energy for creep in J mol^{-1} and R is the gas constant (8.314 J mol^{-1} K^{-1}). Qc^*, k_1 and u parameters are then derivable from a comprehensive data set, although it is important to consider an appropriate explanation for activation energy magnitudes.

In the case of SPC data, the Wilshire equations have been exploited for different means and approaches. Jeffs et al. [22] compared the creep life predictions as determined by the Wilshire equations for SPC results, correlated via the k_{SP} and uniaxial data. This relationship is displayed in **Figure 17**, with a good agreement between each test type seen.

In a similar nature, the Wilshire equations may be modified such that normalisation is carried out using loads rather than stresses [44] as shown in Eq. (8) below:

$$(F/F_m) = \exp\left\{-k_1\left[t_f \exp(-Q_c*/RT)\right]^u\right\} \tag{9}$$

Here, F is the applied SPC test load and F_m the ultimate load through a constant displacement rate SP test. Using such an approach could provide an effective ranking method of material types exclusively through SPC. Alternatively, Holmström et al. [15] has utilised the Wilshire equations to determine a strength correlation factor between weld material variants.

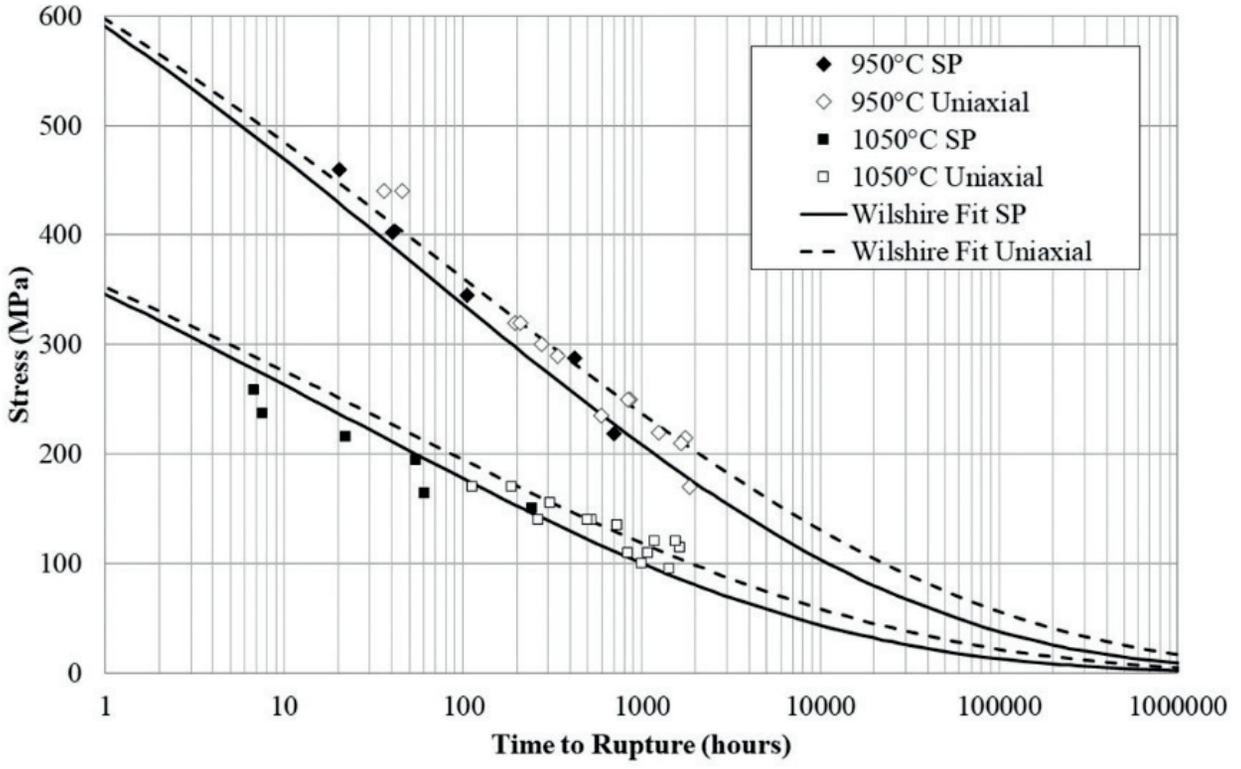

Figure 17. Wilshire equation predictions of σ vs. t_f for uniaxial creep and SPC test types for CMSX-4 [22].

4.3. Numerical approaches

4.3.1. Finite element analysis (FEA)

Several authors have used FEA to predict the SP creep behaviour in different material systems. Evans [45] analysed the SP deformation of 0.5Cr0.5Mo0.25V ferritic steel and assumed deformation was viscoplastic with a constant volume, with deformation rates governed by the creep properties of the material. They used a phenomological constitutive relationship for the creep properties of the internal variable type, where the variables used include hardening, softening and continuum damage with an additional creep failure criterion also adopted. They constructed a model using uniaxial creep data and verified it by comparing the creep curves and t_f from actual SPC tests to those produced through the FEA model, as given in **Figure 18**. As can be seen, the results show good correlation with the FEA model.

Lancaster et al. [23] used a constitutive creep model based on the theta-projection method first developed by Evans [45], which was implemented into Abaqus using a creep derived subroutine. The authors used such an approach to relate creep rate to the accumulation of internal material state variables, which has been previously shown in Ref. [47] to predict creep behaviour better than other strain or time based hardening approaches, for situations where a transient stress state is present, such as in a SPC test. In this research, an axisymmetric model was used to predict the material deformation in a SPC test on γTiAl 45-2-2 (XD) with model geometries replicating those that are used in a SPC experiment, with all features modelled as rigid bodies and surfaces. The model showed that the Von-Mises stress was found to be high across the thickness of the disc and as such, the rate of creep deformation was predicted to be high. However, the maximum principle stress adjacent to the disc was found to be low, but due to a combination of high radial and hoop stresses, the maximum principle stress on the underside of the specimen was high in the central region. As specimen deformation increases with displacement, the stress field is then found to evolve and the peak stress in the disc slowly decreases away from the centre of the disc, leading to the onset of thinning and steady state deformation. An additional damage model dependent on maximum principle stress was incorporated to capture the rupture characteristics of the material and was able to predict rupture to a high level of accuracy when compared to experimental results [23].

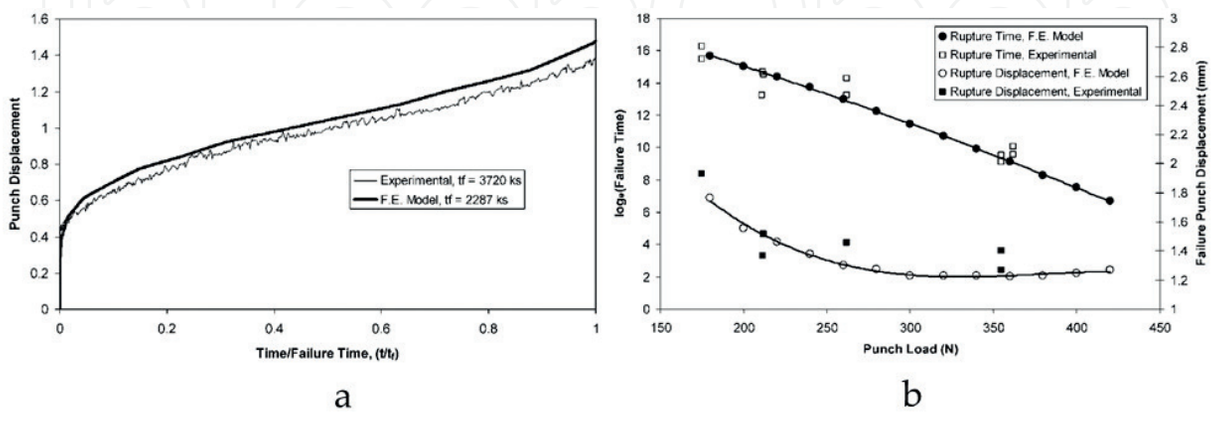

Figure 18. Experimental and modelled SPC results at 848K on 0.5Cr0.5Mo0.25V ferritic steel a. time vs punch displacement for a test performed under 211N and b. failure time vs punch displacement for all simulated and experimental tests [46].

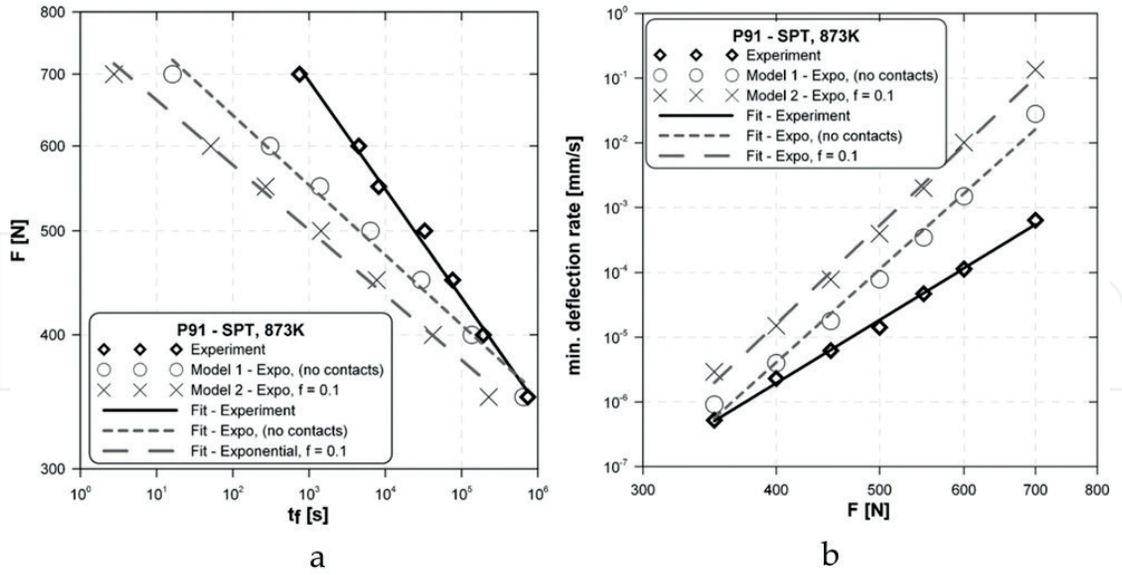

Figure 19. Comparison of results generated from alternative FEA models and experimental SPC tests for P91 steel a. F vs. t_f and b. $\dot{\delta}_M$ vs. F [48].

Dymáček and Milička [48] utilised two basic creep constitutive models, namely Norton power-law ('Model 1') and the exponential relationship ('Model 2'), to run their FEA simulations. Model 1 considered only the simple boundary conditions as supports and assumed the pressure of the load without actually using the specific puncher shape. However, for Model 2, they included contact elements whilst accounting for the surface frictional contact between contacting surfaces. In either case, a simplified 2D axisymmetric model was adopted and the numerical findings from each model were compared with real experimental results, as displayed in **Figure 19**.

The authors found that Model 1 was somewhat limited due to the absence of a friction parameter which was deemed necessary from the research. However, Model 1 was capable of predicting more accurate results under high forces and in general, the values of t_f and $\dot{\delta}_M$ showed good agreement with the experimental data in both models.

Other notable contributions are provided by Nakata et al. [49] for their work on F82H ferritic/martensitic steel; Zhao et al. [13] who simulated the SPC behaviour of P92 steel from several locations around a welded joint; Kobayashi et al. [50] who used FEA to support research into the SPC deformation of aluminium alloys from the duralumin series and Jeffs et al. [22] who adopted ABAQUS to simulate the SPC deformation curves of the single crystal superalloy, CMSX-4.

Author details

Robert J. Lancaster* and Spencer P. Jeffs

*Address all correspondence to: r.j.lancaster@swansea.ac.uk

Swansea University, Swansea, UK

References

[1] Manahan MP, Argon AS, Harling OK. The development of a miniaturizsed disk bend test for determination of post irradiation mechanical properties. Journal of Nuclear Materials. 1981;**104**:1545-50

[2] Manahan MP. A new post-irradiation mechanical behavior test–The miniaturized disk bend test. Nuclear Technology. 1983;**63**(2):295-315

[3] Corwin WR, Lucas GE. The Use of Small-Scale Specimens for Testing Irradiated Material: A Symposium Sponsored by ASTM Committee E-10 on Nuclear Technology and Applications, Albuquerque, N.M., 23 Sept. 1983. [Internet]. ASTM; 1986 [cited 2017 Jun 8]. Available from: https://inis.iaea.org/search/search.aspx?orig_q=RN:18065732

[4] Parker JD, James JD. Disc-bend creep deformation behaviour of 1/2Cr1/2Mo1/4V low alloy steel. In: 5th International Conference: Creep and Fracture of Engineering Materials and Structures, Swansea, Wales: CRC Press, USA; 1993. pp. 651-660

[5] Available from: www.scopus.com. Elsevier B.V

[6] Hyde TH, Sun W, Williams JA. Requirements for and use of miniature test specimens to provide mechanical and creep properties of materials: A review. International Materials Review. 2007;**52**(4):213-255

[7] Kusumoto J, Kanaya A, Kobayashi T. Residual life assessment of 2.25Cr-1Mo boiler pipe by small punch creep test. In: ASME 2006 Pressure Vessels and Piping/ICPVT-11 Conference; Vancouver, BC: ASME, USA; 2006. pp. 637-642

[8] Ule B, Šuštar T, Dobeš F, Milička K, Bicego V, Tettamanti S, et al. Small punch test method assessment for the determination of the residual creep life of service exposed components: Outcomes from an interlaboratory exercise. Nuclear Engineering and Design. 1999;**192**(1):1-11

[9] Izaki T, Kobayashi T, Kusumoto J, Kanaya A. A creep life assessment method for boiler pipes using small punch creep test. International Journal of Pressure Vessels and Piping, [Internet]. Elsevier Ltd; 2009;**86**(9):637-642. Available from: http://dx.doi.org/10.1016/j.ijpvp.2009.04.005

[10] Rolls-Royce Power Engineering plc. Scoop sampling – Extraction of material samples for examination and analysis [Internet]. Commissioning and In-service Support; 2010. [Online]. Available from: http://www.rolls-royce.com/~/media/Files/R/Rolls-Royce/documents/customers/nuclear/scoop-sampling-tcm92-50918.pdf

[11] Omacht D, Kubanek Z, Dolezal R. Development of testing machines and equipment for small punch testing, proposals for improvement of CWA 15627. Key Engineering Materials [Internet]. 2017;**734**:237-248. Available from: http://www.scientific.net/KEM.734.237

[12] Kumar K, Madhusoodanan K, Rupani BB. Miniature specimen technique as an NDT tool for estimation of service life of operating pressure equipment. International Conference of Pressure Vessels and Piping, OPE-2006-Chennai, Chennai, India: BARC Newsletter, India; 2006. p. 92-102

[13] Zhao L, Jing H, Xu L, Han Y, Xiu J, Qiao Y. Evaluating of creep property of distinct zones in P92 steel welded joint by small punch creep test. Materials and Design [Internet]. 2013;**47**:677-686 Available from: http://dx.doi.org/10.1016/j.matdes.2012.12.032

[14] Gülçimen B, Hähner P. Determination of creep properties of a P91 weldment by small punch testing and a new evaluation approach. Materials Science and Engineering A [Internet]. Elsevier; 2013;**588**:125-131. Available from: http://dx.doi.org/10.1016/j.msea.2013.09.029

[15] Holmström S, Auerkari P, Hurst R, Blagoeva D. Using small punch test data to determine creep strain and strength reduction properties for heat affected zones. Materials Science and Technology [Internet]. 2014;**30**(1):63-66. Available from: http://www.maneyonline.com/doi/abs/10.1179/1743284713Y.0000000311

[16] Kim B, Lim B. Local creep evaluation of P92 steel weldment by small punch creep test. Acta Mechanica Solida Sinica [Internet]. The Chinese Society of Theoretical and Applied Mechanics; 2008;**21**(4):312-317. Available from: http://dx.doi.org/10.1007/s10338-008-0836-z

[17] Jeffs S, Lancaster R, Davies S. Effect of build orientation and post processing of a direct laser deposited nickel superalloy as determined by the small punch creep test. Key Engineering Materials. 2017;**734**:128-136

[18] Bruchhausen M, Turba K, De Haan F, Hähner P, Austin T, De Carlan Y. Characterization of a 14Cr ODS steel by means of small punch and uniaxial testing with regard to creep and fatigue at elevated temperatures. Journal of Nuclear Materials [Internet]. Elsevier B.V.; 2014;**444**(1–3):283-291. Available from: http://dx.doi.org/10.1016/j.jnucmat.2013.09.059

[19] Turba K, Hurst RC, Hähner P. Anisotropic mechanical properties of the MA956 ODS steel characterized by the small punch testing technique. Journal of Nuclear Materials [Internet]. Elsevier B.V.; 2012 Sep;**428**(1–3):76-81. Available from: http://linkinghub.elsevier.com/retrieve/pii/S0022311511008191

[20] Mathew MD, Ganesh Kumar J, Ganesan V, Laha K. Small punch creep studies for optimization of nitrogen content in 316LN SS for enhanced creep resistance. Metallurgical and Materials Transactions A, Physical Metallurgy and Materials Science. 2014;**45**(2):731-737

[21] Jeffs SP, Lancaster RJ. Elevated temperature creep deformation of a single crystal superalloy through the small punch creep method. Materials Science and Engineering A. 2015 Feb;**626**:330-337

[22] Jeffs SP, Lancaster RJ, Garcia TE. Creep lifing methodologies applied to a single crystal superalloy by use of small scale test techniques. Materials Science and Engineering A. 2015;**636**:529-535

[23] Lancaster RJ, Harrison WJ, Norton G. An analysis of small punch creep behaviour in the γ titanium aluminide Ti-45Al-2Mn-2Nb. Materials Science and Engineering A. 2015 Feb;**626**:263-274

[24] Andrés D, Lacalle R, Álvarez JA. Creep property evaluation of light alloys by means of the small punch test: Creep master curves. Materials and Design [Internet]. Elsevier Ltd; 2016;**96**:122-130. Available from: http://dx.doi.org/10.1016/j.matdes.2016.02.023

[25] Kumar JG, Laha K. Small punch creep deformation and rupture behavior of 316L (N) stainless steel. Materials Science and Engineering A [Internet]. Elsevier; 2015;**641**:315-322. Available from: http://dx.doi.org/10.1016/j.msea.2015.06.053

[26] CEN Workshop Agreement CWA 15267. European Code of Practise: Small Punch Test Method for Metallic Materials. CEN Members National Standards Body; 2007. p. 1-69

[27] Matocha K, Hurst R. Small punch testing–The transition from a code of practice to a European testing standard. Key Engineering Materials [Internet]. 2017;**734**:3-22. Available from: http://www.scientific.net/KEM.734.3

[28] Naveena, Komazaki S. Evaluation of creep rupture strength of high nitrogen ferritic heat-resistant steels using small punch creep testing technique. Materials Science and Engineering: A [Internet]. Elsevier; 2016;**676**:100-108. Available from: http://dx.doi.org/10.1016/j.msea.2016.08.102

[29] Chakrabarty J. A theory of stretch forming over hemispherical punch heads. International Journal of Mechanical Sciences. 1970;**12**:315-325

[30] Yang Z, Wen Wang Z. Relationship between strain and central deflection in small punch creep specimens. International Journal of Pressure Vessels and Piping. 2003;**80**(6):397-404

[31] Li Y, Šturm R. Determination of creep properties from small punch test. In: ASME 2008 Pressure Vessels and Piping Conference. Chicago, IL: ASME, USA; 2008. pp. 739-750

[32] Rouse JP, Cortellino F, Sun W, Hyde TH, Shingledecker J. Small punch creep testing: review on modelling and data interpretation. Materials Science and Technology [Internet]. 2013 Nov;**29**(11):1328-1345. Available from: http://www.maneyonline.com/doi/abs/10.1179/1743284713Y.0000000278

[33] Blagoeva DT, Hurst RC. Application of the CEN (European Committee for Standardization) small punch creep testing code of practice to a representative repair welded P91 pipe. Materials Science and Engineering A. 2009;**510–511**(C):219-223

[34] Monkman FC, Grant NJ. An empirical relationship between rupture life and minimum creep rate in creep-rupture tests. Proceedings of ASTM International. 1956;**56**:593-620

[35] Dobeš F and Milička K. Application of creep small punch testing in assessment of creep lifetime. Materials Science and Engineering: A. 2009 Jun;**510–511**:440-443

[36] Dymáček P. Recent developments in small punch testing: Applications at elevated temperatures. Theoretical and Applied Fracture Mechanics. 2016;**86**:25-33

[37] Evans RW, Wilshire B. Creep of Metals and Alloys. London, UK: The Institue of Metals; 1985. 197-243 p.

[38] Law M, Payten W, Snowden K. Modelling creep of pressure vessels with thermal gradients using theta projection data. International Journal of Pressure Vessels and Piping. 2002;**79**(12):847-851

[39] Zheng Y, Yang S, Ling X. Creep life prediction of small punch creep testing specimens for service-exposed Cr5Mo using the theta-projection method. Engineering Failure Analysis

[Internet]. Elsevier Ltd; 2017;**72**:58-66. Available from: http://dx.doi.org/10.1016/j.engfailanal.2016.11.009

[40] Yang S, Ling X, Zheng Y. Creep behaviors evaluation of Incoloy800H by small punch creep test. Materials Science and Engineering A [Internet]. Elsevier; 2017;**685**(Nov 2016):1-6. Available from: http://dx.doi.org/10.1016/j.msea.2016.12.092

[41] Whittaker MT, Evans M, Wilshire B. Long-term creep data prediction for type 316H stainless steel. Materials Science and Engineering A [Internet]. Elsevier B.V.; 2012;**552**:145-150. Available from: http://linkinghub.elsevier.com/retrieve/pii/S0921509312007150

[42] Wilshire B, Battenbough AJ. Creep and creep fracture of polycrystalline copper. Materials Science and Engineering A [Internet]. 2007 Jan;**443**(1–2):156-166. Available from: http://linkinghub.elsevier.com/retrieve/pii/S0921509306019460

[43] Wilshire B, Scharning PJ. Long-term creep life prediction for a high chromium steel. Scripta Materialia [Internet]. 2007 Apr;**56**(8):701-704. Available from: http://linkinghub.elsevier.com/retrieve/pii/S1359646207000231

[44] Holmström S, Hähner P, Hurst RC, Bruchhausen M, Fischer B, Lapetite J-M, et al. Small punch creep testing for material characterization and life time prediction. Materials for Advanced Power Engineering. Juelich, Germany: FZ. Juelich, Germany; 2014. pp. 627-635

[45] Evans RW. A constitutive model for the high-temperature creep of particle-hardened alloys based on the θ projection method. Proc R Soc A Math Phys Eng Sci. 2000;**456**:835-68

[46] Evans RW, Evans M. Numerical modelling of small disc creep test. Materials Science and Technology. 2006;**22**(June):1155-1162

[47] Harrison WJ, Whittaker MT, Deen C. Creep behaviour of Waspaloy under non-constant stress and temperature. Materials Research Innovations. 2013;**17**(5):323-326

[48] Dymáček P, Milička K. Creep small-punch testing and its numerical simulations. Materials Science and Engineering A [Internet]. 2009 Jun;**510–511**:444-449. Available from: http://linkinghub.elsevier.com/retrieve/pii/S0921509308014780

[49] Nakata T, Komazaki S, Kohno Y, Tanigawa H. Development of a small punch testing method to evaluate the creep property of high Cr ferritic steel: Part II–Stress analysis of small punch test specimen by finite element method. Materials Science and Engineering A [Internet]. Elsevier; 2016;**666**:80-87. Available from: http://dx.doi.org/10.1016/j.msea.2016.03.102

[50] Kobayashi K, Kajihara I, Koyama H, Stratford GC. Deformation and fracture mode during small punch creep tests. Journal of Solid Mechanics and Materials Engineering. 2010;**4**(1):75-86